Hop2-Mnd1 Condenses DNA to Stimulate the Synapsis Phase of DNA Strand Exchange

Roberto J. Pezza,[†] R. Daniel Camerini-Otero,[†] and Piero R. Bianco[‡*]
[†]Genetics and Biochemistry Branch, National Institute of Diabetes and Digestive and Kidney Diseases, National Institutes of Health, Bethesda, Maryland; and [‡]Center for Single Molecule Biophysics, Department of Microbiology and Immunology, University at Buffalo, Buffalo, New York

ABSTRACT Hop2-Mnd1 is a meiotic recombination mediator that stimulates DNA strand invasion by both Dmc1 and Rad51. To understand the biochemical mechanism of this stimulation, we directly visualized the heterodimer acting on single molecules of duplex DNA using optical tweezers and video fluorescence microscopy. The results show that the Hop2-Mnd1 heterodimer efficiently condenses double-stranded DNA via formation of a bright spot or DNA condensate. The condensation of DNA is Hop2-Mnd1 concentration-dependent, reversible, and specific to the heterodimer, as neither Hop2 nor Mnd1 acting alone can facilitate this reaction. The results also show that the rate-limiting nucleation step of DNA condensation is overcome in the presence of divalent metal ions, with the following order of preference: $Mn^{2+}>Mg^{2+}>Ca^{2+}$. Hop2-Mnd1/Dmc1/single-stranded DNA nucleoprotein filaments also condense double-stranded DNA in a heterodimer concentration-dependent manner. Of importance, the concentration dependence parallels that seen in DNA strand exchange. We propose that rapid DNA condensation is a key factor in stimulating synapsis, whereas decondensation may facilitate the invasion step and/or the ensuing branch migration process.

INTRODUCTION

Homologous recombination serves a critical function in the repair of DNA double-strand breaks (DSBs) in mitosis and in the proper segregation of homologous chromosomes in meiosis (1,2). Programmed DSBs force homologous chromosomes to undergo recombination resulting in crossover formation, which is essential for proper chromosome disjunction at the first meiotic division (3,4). The recombinases Dmc1 and Rad51 are loaded onto resected DSBs and subsequently promote the search for homology and catalyze DNA strand invasion (3–10).

Several studies have demonstrated that Hop2 and Mnd1 are indispensable for meiotic recombination (11–15). In the absence of these proteins in vivo, Dmc1 or Rad51 is loaded onto the resected DSBs but further progression of recombination is impaired. Hop2 and Mnd1 form a heterodimer that stimulates in vitro DNA strand exchange mediated by Dmc1 and Rad51 (13,16–21). Hop2-Mnd1 binds to either Dmc1 or Rad51, stabilizes the respective nucleoprotein filaments, and enhances the capture of double-stranded DNA (dsDNA) into filaments in a homology-independent manner (20,21). The combination of these two activities leads to a significant enhancement in DNA strand exchange by either recombinase (13,16,17). The mechanism of this stimulation is unknown and therefore is the focus of this work.

Submitted July 19, 2010, and accepted for publication October 19, 2010.

*Correspondence: pbianco@buffalo.edu

Roberto J. Pezza's present address is Cell Cycle and Cancer Biology Research Program, Oklahoma Medical Research Foundation, Oklahoma City, Oklahoma.

Editor: David P. Millar.

0006-3495/10/12/3763/10 $2.00

MATERIALS AND METHODS

Proteins

Purification and refolding of recombinant Mnd1

Murine *MND1* was purified as a protein linked to a histidine tag on the amino terminus. The protein was overexpressed in *Escherichia coli* BL21 (DE3). The cells were grown to an *A*600 of 0.6–0.8, and Mnd1 synthesis was induced by the addition of 1 mM IPTG for 2 h at 37°C. Cells were then harvested by centrifugation, washed in chilled buffer (20 m MHEPES (pH 8.0), 100 mM NaCl, and 5 mM EDTA), resuspended in lysis buffer (20 m MHEPES (pH 8.0), 100 mM NaCl, 0.5% Triton, 5 mM EDTA, lysozyme 200 μg/mL, and protease inhibitors; Roche Applied Science, Indianapolis, IN), and lysed by sonication. Inclusion bodies were collected by centrifugation at 18,000 $\times$ *g* at 4°C and washed in lysis buffer without EDTA and lysozyme, and once in the following buffer: 20 mM HEPES (pH 8.0), 10% glycerol, 0.5 M NaCl, and protease inhibitors. Next, inclusion bodies were solubilized overnight with agitation in 50 mM HEPES (pH 8.0), 0.5 M NaCl, 10% glycerol, and 1.8 M guanidine hydrochloride. Solubilized inclusion bodies were centrifuged for 30 min at 18,000 *g*, the supernatant was diluted 20–40 times in refolding solution (500 mM NaCl, 50 mM HEPES (pH 8.0), 10% glycerol), and the refolding was allowed to proceed for 15 h at 4°C. The solution containing the refolded protein was centrifuged for 30 min at 8,000 $\times$ *g* and loaded onto a nickel-nitrilotriacetic acid column that was previously equilibrated with refolding buffer. The column was washed with five volumes of refolding buffer, and bound protein was eluted with 500 mM imidazole. The peak corresponding to Mnd1 was loaded onto hydroxyapatite (Bio-Gel HT gel; Bio-Rad, Hercules, CA) and washed with 10 column volumes of washing buffer (300 mM NaCl, 50 mM HEPES (pH 8.0), glycerol 10%). The protein was then eluted with a 100-mL linear gradient (0–300 mM) of phosphate buffer prepared in washing buffer. Finally, Mnd1 was concentrated by ultrafiltration (centripep YM-10; Amicon, Billerica, MA) and loaded on Superdex 200 (HP16/60; GE Healthcare, Piscataway, NJ) in 50 mM HEPES (pH 8.0), 300 mM NaCl, and 10% glycerol. Fractions corresponding to the protein peak were pooled, concentrated with Centripep YM-10 (Millipore, Billerica, MA), and stored in aliquots at −80°C.

doi: 10.1016/j.bpj.2010.10.028

Expression and purification of recombinant Hop2 and the Hop2-Mnd1 complex

HOP2 or *HOP2* and *MND1* together were cloned in a pET-15b vector (Novagen, Gibbstown, NJ) to generate a protein linked to a histidine tag on the amino terminus (only Hop2 was His-tagged in the Hop2-Mnd1 complex). The proteins were overexpressed in *E. coli* BL21 (DE3) and purified using the following series of chromatographic steps: nickel-nitrilotriacetic acid-agarose (Qiagen, Valencia, CA), hydroxyapatite (Bio-Gel HT Gel, Bio-Rad), Mono Q, and Superdex 200. The proteins were concentrated and stored in buffer (20 mM Tris-HCl (pH 7.4), 300 mM NaCl, 10% glycerol) at −80°C.

Purification of human Dmc1 protein

Recombinant hDmc1 protein was purified from 6 liters of *E. coli* FB850 *recA* mutant pLysS carrying plasmid pET15b-Dmc1 grown at 30°C in tryptone phosphate medium supplemented with 100 μg of ampicillin/mL and 25 μg of chloramphenicol/mL. At an optical density at 600 nm (OD 600) of 0.5, hDmc1 synthesis was induced by the addition of 0.5 mM IPTG and incubation at 25°C. After 12 h, the cells were harvested by centrifugation, frozen in dry ice, and stored at −80°C. The cell paste was resuspended in 200 mL of lysis buffer (0.1 M Tris-Cl (pH 8.0), 10% glycerol, 0.1% Triton X-100, 500 mM NaCl, and 10 mM imidazole) containing the protease inhibitors phenylmethylsulfonyl fluoride (1 mM), aprotinin (0.019 trypsin inhibitor unit (TIU)/mL), leupeptin (1 μg/mL), and pepstatin A (1 μg/mL). The suspension was divided into 40-mL aliquots that were sonicated three times for 1 min. Insoluble material was removed by centrifugation at 50,000 rpm for 30 min. The supernatant containing Dmc1 was loaded on a 10-mL Ni-column (Invitrogen, Carlsbad, CA). The column was washed successively with 200 and 160 mL of T buffer containing 30 and 50 mM imidazole, respectively, before Dmc1 was eluted with a 160-mL linear gradient of 0.04–0.5 M imidazole in T buffer. Fractions of Dmc1, which eluted as a broad peak, were identified by sodium dodecyl sulfate-polyacrylamide gel electrophoresis, pooled, and equilibrated against R buffer (50 mM Tris-HCl (pH 8.0), 10% glycerol, 0.5 mM DTT) containing 100 mM NaCl and loaded onto a 20-mL Heparin Fastflow column (Pharmacia, Piscataway, NJ). The column was washed with 200 mL of R100, and Dmc1 was eluted with a 160-mL linear gradient of 0.1–1 M KCl in R buffer. Dmc1was loaded directly onto a 1-mL MonoQ column (HR 5/5) by means of a Pharmacia FPLC system. The column was washed with 20 mL of R100 before hDmc1 was eluted by using a linear gradient of 10 mL of 0.1–1.0 M KCl in R buffer. Dmc1 eluted in a sharp peak at 0.5 M KCl. The protein was equilibrated against 1 liter of S buffer (20 mM Tris-acetate (pH 7.5), 0.35 M sodium chloride, 10% glycerol, 0.5 mM DTT) and stored in aliquots at −80°C. The concentration of Dmc1 was determined by Bradford assay.

DNA

M13 mp7 single-stranded DNA (ssDNA) was purified as described previously (22). All other DNA substrates were obtained from New England Biolabs (Ipswich, MA).

Coaggregate assay

The reactions (30 μL, 37°C) contained 20 mM Tris-OAc (pH 7.5), 0.1 mg/mL bovine serum albumin, 1 mM DTT, 20% sucrose, 20 U/mL of pyruvate kinase, 15 mM PEP, 1 mM $Mg(OAc)_2$, 1 mM $CaCl_2$, 10 μM nts ϕX174 ssDNA, 3 μM Dmc1 or Rad51, 1.2 μM Hop2-Mnd1, and 116 μM nts linear, heterologous pPB322. Reactions were initiated by adding Dmc1 or Rad51 to the ssDNA and incubating the sample for 15 min, followed by incubation with Hop2-Mnd1 (5 min) and dsDNA (10 min). Reaction processing was performed as described previously (23) (Fig. 1 *A*).

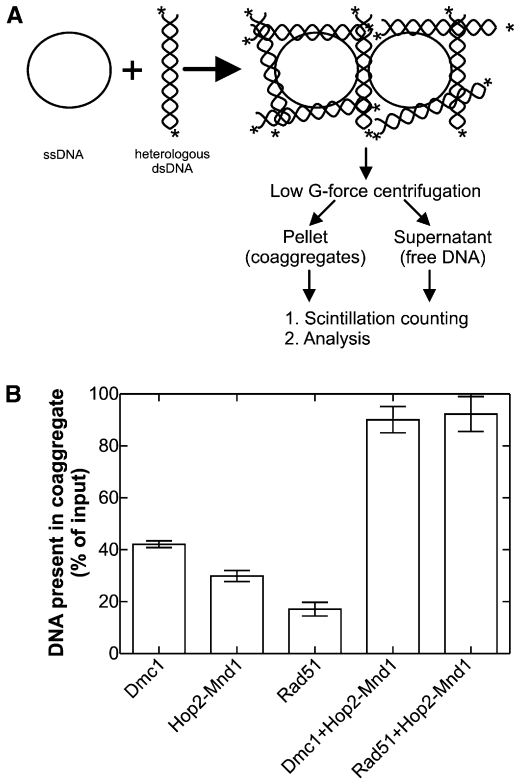

FIGURE 1 Hop2-Mnd1 stimulates formation of DNA networks. (*A*) Schematic of the bulk-phase coaggregate assay (30). The single-stranded circular DNA was ϕX174 ssDNA, and the heterologous, linear dsDNA was 5′-end-labeled, pPB322. * = ^{32}P. (*B*) Analysis of bulk-phase coaggregate assays done in triplicate (23,30).

Optical trapping and video fluorescence microscopy

Reactions were performed in two-stream, micromachined flow cells with inlet ports connected to 1 mL Hamilton gas-tight syringes controlled by a syringe pump (PHD 2000; Harvard Apparatus, Holliston, MA). Flow cells were held in place on a Märzhäuser stage in a Leica DMIRE2 fluorescence microscope (Leica, Bannockburn, IL). The DMIRE2 was modified to mate with a laser manipulator (LM-02; Solar TII, Minsk, Belarus) containing galvano-scanning mirrors (VM500; GSI Lumonics, Billerica, MA). Optical traps were formed by passing an Nd:YVO_4 infrared laser (wavelength = 1064 nm, 5W; Spectra Physics, Irvine, CA) through the LM-02, which split the beam into S- and P-components to form fixed and mobile optical traps in the focal plane of the microscope. The position and motion of the mobile trap were controlled by the scanning mirrors. The resulting independent laser beams were focused through an oil-immersion objective lens (Plan Apo 100×, 1.4 NA; Leica) to a position 18 μm above the lower surface of the flow cell. Fluorescent DNA-bead complexes were excited with an XCite120 lamp (XFO) using a GFP-3035B fluorescence cube (Semrock, Rochester, NY). Fluorescence images were captured at video rate by an EB-CCD camera (Hamamatsu) and recorded on digital videotape (DV184) with a digital VCR (DSR-11; Sony, Tokyo, Japan).

DNA-bead preparation and single DNA molecule reactions

DNA-bead complexes were prepared as described previously (23). Sample syringes contained 30 mM sodium bicarbonate (pH 8), 100 mM DTT, 20%

sucrose, 9.9×10^7 DNA-bead complexes, and 0.2 μM YOYO-1. Reaction syringes contained 30 mM Tris-acetate (pH 7.5), 30 mM DTT, 20% sucrose, 100 nM Hop2-Mnd1 (standard condition), and other components as indicated in Table 1 and the figure legends. Reactions were done at 23°C at a linear flow velocity of 74 μm/s. For reactions in which nucleoprotein filaments were present in the reaction channel, filaments were assembled as follows: M13 ssDNA was added to the reaction buffer, followed by Dmc1, and the mixture was incubated for 5 min. Hop2-Mnd1 was added and allowed to bind for 5 min before being introduced into the syringe.

Data analysis

Movies were downloaded to an IBM-compatible computer and subsequent data analyses were performed as follows: Images were captured on an IBM-compatible computer interfaced with the DSR-11 via a PIXCI SV5 frame-grabber controlled by XCAP software (EPIX). Captured videos were converted into individual sequential frames to obtain measurements using Image-Pro Plus v6.1 (Media Cybernetics, Bethesda, MD). The microscope optics was calibrated with a Stage Micrometer (Leica), resulting in 8.54 pixels per micron. Under the assay conditions used, the average corrected length of individual, stretched, fluorescent λ DNA molecules was 18 μm ($n = 100$). DNA lengths were corrected for slight bead blooming (i.e., beads appeared 1.2× larger than anticipated). Thus for all calculations, given that λ DNA is 48,504 basepairs (bp) long, the average number of bp/μm was 2695.

We calculated the rate of DNA condensation by measuring the observed length of DNA in each frame of a time course, and using the object-tracking function of Image Pro to track the position of bright spots as a function of time. Data were exported from Image Pro and analyzed with the use of GraphPad Prism (v 5.1). Before bright spot formation occurred, we measured the DNA length using the length measurement tool of Image Pro. Once bright spots were detected, we monitored their position using the object-tracking function of Image Pro. Overlapping data sets of DNA length and bright spot position were combined to yield complete trajectories. Lag times were determined as follows: First, a linear fit to the steady-state portion of the time course was obtained. This line was extrapolated to zero position. The intercept on the abscissa corresponds to the lag time for bright spot formation.

To ascertain the time-dependent position of DNA condensates (bright spots), we smoothed the data from individual trajectories with a second-order Savitzky-Golay filter with a time constant of 0.2 s as described previously (23,24). We then determined the instantaneous velocity for each bright spot by using a differential average over the length of the movie from the point at which bright spots were observed until they either ceased moving entirely (2% of molecules) or encountered the bead (98% of DNA molecules). The instantaneous velocities were then averaged to obtain the steady-state condensation rate.

The analysis of binding constants was done as described previously (25–27). The on-rate, k_{on}, was determined as follows: To determine the rate of heterodimer binding, the steady-state rate of condensation was divided by the site size of 3.16 for the Hop2-Mnd1 heterodimer (18). This value was then divided by the protein concentration to provide the on-rate. The off-rate was determined by dividing the decondensation rate by the site size. Finally, the dissociation constant K_d was determined by dividing the off-rate by the on-rate, $K_d = k_{off}/k_{on}$.

TABLE 1 Hop2-Mnd1 DNA condensation parameters

Reaction condition	No. movies analyzed	Condensation rate (bp/s)[§]	Average lag time (s)
Protein dependence*			
50 nM Hop 2	10	No reaction	-
100 nM Hop2	10	No reaction	-
50 nM Mnd1	10	No reaction	-
100 nM Mnd1	10	No reaction	-
1 nM Hop2-Mnd1 (H-M)	3	No reaction	-
10 nM H-M	4	No reaction	-
50 nM H-M	12	11,144 ± 7087	4.10
100 nM H-M	24	33,089 ± 14,087	0.73
200 nM H-M	3	25,296 ± 7953	0.90
300 nM H-M	7	17,415 ± 7569	1.44
600 nM H-M	11	35,768 ± 6275	0.17
Effects of Dmc1 and/or M13 ssDNA[†]			
300 nM H-M+ 2.5 μM M13 ssDNA	5	18,016 ± 7844	0.16
600 nM H-M + 5 μM M13 ssDNA	10	35,625 ± 6595	0.17
1.5 μM Dmc1	18	No reaction	-
1.5 μM Dmc1 + 3 μM M13	20	No reaction	-
1.5 μM Dmc1 + 3 μM M13 + 50 nM H-M	18	1 DNA condensed	-
1.5 μM Dmc1 + 3 μM M13 + 200 nM H-M	10	15,513 ± 7528	1.03
1.5 μM Dmc1 + 3 μM M13 + 600 nM H-M	10	38,014 ± 14,847	0.00[¶]
1.5 μM Dmc1 + 3 μM M13 + 1200 nM H-M	10	14,107 ± 4666	0.00[¶]
Metal ion present[‡]			
$MnCl_2$	9	45,580 ± 10,093	0.00[¶]
MgOAC	15	34,068 ± 8962	0.23
MgOAC + ATP	11	29,170 ± 5803	0.62
$CaCl_2$	9	24,210 ± 7783	0.28
None	12	8590 ± 2543	1.20

*Reactions contained 2.5 mM MgOAc only.

[†]Reactions contained 2.5 mM MgOAc, 2 mM ATP (to mimic strand invasion conditions).

[‡][metal ion] = 2.5 mM and 2 mM ATP (where indicated); 125 nM Hop2-Mnd1.

[§]The error reflects the differences in rate observed between different DNA molecules in each data set.

[¶]A lag of 0 s indicates a lag that was too rapid to be precisely determined.

RESULTS AND DISCUSSION

Hop2-Mnd1 stimulates DNA network formation

Previous work showed that the mitotic recombination mediator Rad54 stabilizes Rad51 nucleoprotein filaments and stimulates Rad51-mediated DNA network formation (23,28). DNA networks, which are intermediates on the pathway to product formation, contain coaggregates of nucleoprotein filaments bound to multiple dsDNA molecules simultaneously (23) (Fig. 1 *A*). Stimulation of these networks by Rad54 involves a combination of dsDNA capture and ATP hydrolysis-coupled dsDNA translocation, resulting in an overall enhancement in DNA strand exchange similar to that observed for the *E. coli* RecA protein (29). Of note, RecA efficiently catalyzes DNA network formation in the absence of accessory proteins (30).

The meiotic recombination mediator Hop2-Mnd1 facilitates the capture of dsDNA into Dmc1 or Rad51 nucleoprotein filaments (20,21). To determine whether capture is followed by DNA network formation, we performed coaggregate assays using heterologous DNA to permit capture but block the subsequent DNA strand invasion and exchange phases of the reaction (23,30).

The control assays showed that Dmc1, Rad51, and Hop2-Mnd1 alone are relatively inefficient in stimulating DNA network formation (Fig. 1 *B*). The addition of a stoichiometric amount of Hop2-Mnd1 relative to recombinase resulted in a 2.5-fold stimulation of DNA networks by Dmc1, and a 5-fold stimulation by Rad51. In both cases, 95% of the dsDNA present was incorporated into coaggregates, in similarity to previous findings for RecA (30). Further, Hop2-Mnd1 is as effective as Rad54 in stimulating DNA networks by Rad51 (23). Therefore, both Hop2-Mnd1 and Rad54 facilitate dsDNA capture into recombinase filaments, leading to a significant enhancement in the formation of DNA networks.

Hop2-Mnd1 rapidly condenses DNA

Of critical importance is the fact that ATP is required for the mediator function of Hop2-Mnd1 but not for Rad54 (13,18,31,32). Therefore, these two mediators must employ different mechanisms to stimulate the DNA networks, as proposed previously (13). To determine whether this is correct, and because the coaggregate assay is complex (involving multiple, concurrent interactions), we utilized a single DNA molecule technique to gain detailed insight into the biochemical mechanism of Hop2-Mnd1 (23). To that end, we visualized the interaction of Hop2-Mnd1 on isolated, single molecules of λ DNA in real time under conditions that preclude intermolecular aggregation.

DNA substrates were constructed as described previously (23) and then attached at low density to 1 μm streptavidin-coated polystyrene beads. The fluorescent dye YOYO-1 was bound to the DNA, and the fluorescent-labeled, single molecules of DNA were optically trapped and fluid-stretched in the first stream of a Y-shaped, microfluidic, laminar flow cell (Fig. 2 *A*) (23,27,33). Reaction buffer containing Hop2-Mnd1 was introduced into the second stream under conditions of laminar flow, creating a situation in which the two streams flowed parallel to one another with minimal mixing. Once a λ-DNA-bead complex was trapped, the stage was moved so that the complex could be translated from the sample to the reaction stream of the flow cell, and reactions could be initiated in a controlled and precise fashion.

Surprisingly, the anticipated binding of Hop2-Mnd1 to individual DNA molecules resulted in a rapid and efficient DNA condensation reaction (Fig. 2, *B* and *C*). The reaction shown in Fig. 2 consists of several phases dictated by the position of the trapped complex in the fluid streams. Before stage translation occurs, the DNA is fully stretched in the sample fluid stream and the length remains constant (first 1 s of Fig. 2 *C*). During lateral translation, the DNA molecule shortens to slightly less than 48,504 bp as the stretching force is decreased (between arrows 1 and 2) (34). As the interstream boundary is approached, the translation speed is increased to facilitate a more rapid transition into the reaction stream. Consequently, the DNA molecule length decreases more rapidly (between arrows 2 and 3). Once the DNA molecule enters the protein stream (at arrow 3), a further increase in the rate of DNA shortening occurs, lasting 0.4 s. During this time period, the initial binding of Hop2-Mnd1 leading to formation of a bright spot at the free DNA end distal to the bead occurs (arrow 2 in Fig. 2 *B* and arrow 4 in Fig. 2 *C*). Once the bright spot has formed, further DNA condensation takes place, with the spot moving rapidly toward the bead at a rate of 42,172 $\pm$ 813 bp/s, concomitant with a linear increase in its size (data not shown). The bright spot observed here is strikingly similar to toroids formed on single molecules of DNA during their condensation by protamine (27). For simplicity, and because we cannot rigorously demonstrate in this work that the bright spot is a toroid, we define the bright spot as a DNA condensate. This structure consists of DNA and Hop2-Mnd1 heterodimers bound in close proximity so as to facilitate DNA condensation (18).

The condensation trajectory is punctuated by several pauses at 2.5, 2.9, and 3.1 s (Fig. 2 *C*). The pauses are sequence-independent, as they are observed at different positions on the DNA in separate reactions (data not shown). Further, the frequency of pausing decreases as the concentration of Hop2-Mnd1 increases (data not shown). We attribute these pauses to the DNA condensate encountering regions of DNA that are incompletely covered by Hop2-Mnd1. Because the DNA condensation is protein-dependent (see below), the condensation structure pauses when it encounters naked DNA. This allows additional heterodimer to bind, enabling condensation to resume. DNA condensation with a bright spot forming at the free end of the DNA

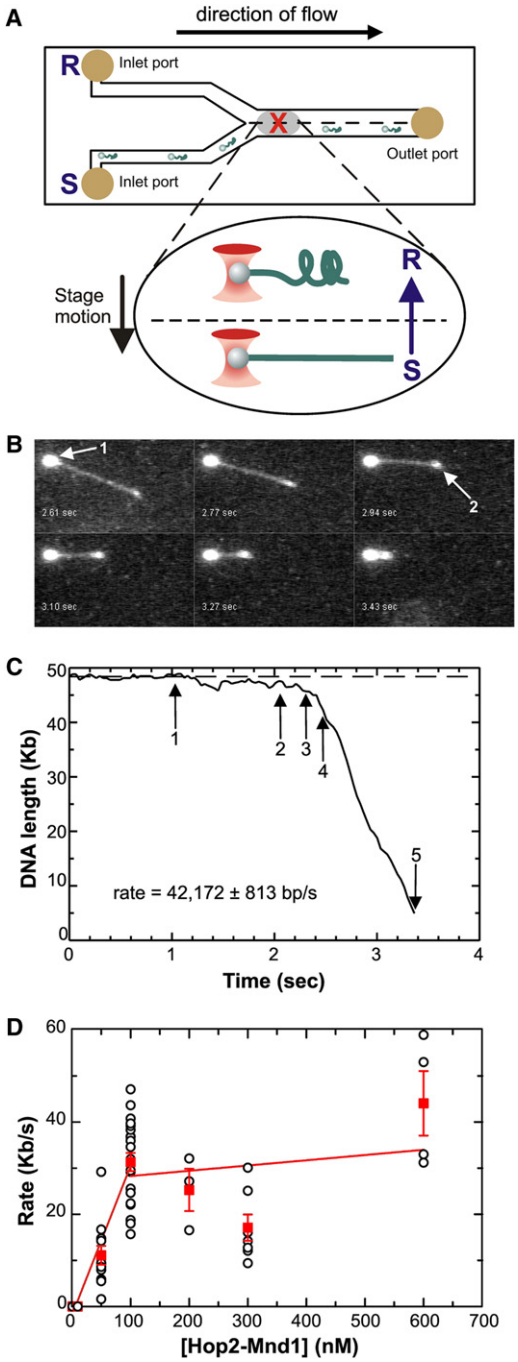

FIGURE 2 Hop2-Mnd1 rapidly condenses DNA. (*A*) A schematic showing optically trapped and fluid-stretched DNA within a flow cell (not to scale). The positions of the trapped DNA molecules are highlighted by the gray-shaded sphere in the center of the flow cell. The X indicates the position of the trap. The arrow above the flow cell indicates the direction of flow and the direction in which the attached DNA molecules are stretched. The arrow to the left of the inset indicates the direction the motorized stage is moved once a DNA-bead complex has been trapped. The result of this motion is to translate the trapped DNA (*green strand*, *inset*) from the sample (S) to the reaction stream (R) of the flow cell, where it can be condensed (indicated as shortening of the dsDNA concomitant with DNA condensate formation). (*B*) Selected frames from a video recording of DNA condensation in the presence of 100 nM Hop2-Mnd1 and 2.5 mM MgOAc. Fluid flow is from left to right, resulting in DNA extension. The optically trapped bead is visible as a large white sphere (*arrow 1*) and the DNA is shown as a white string. The direction of condensation is right to left (i.e., from the DNA end opposite the bead, toward the bead). Condensation results in the formation of a bright spot or DNA condensate (*arrow 2*) that moves rapidly toward the bead as the DNA molecule is condensed further. Numbers at the bottom left of each frame indicate elapsed time. Because the reaction is rapid, the bright spot in the frames shown appears blurred. This is an artifact of montage creation and does not affect object tracking (data not shown). (*C*) Analysis of the time course in *B*. The dashed line demarcates full-length λ DNA. Arrow 1: Interstream motion initiates. Arrow 2: The translation speed increases as the interstream boundary is approached. Arrow 3: The reaction stream is entered. Arrow 4: DNA condensate forms. Arrow 5: Condensation ceases when the bead is encountered. The rate is the steady-state rate of condensation determined between arrows 4 and 5, as described in the Materials and Methods. (*D*) DNA condensation is dependent on the concentration of Hop2-Mnd1. The analysis of DNA condensation reactions done in the presence of different concentrations of Hop2-Mnd1 is shown. Reactions were done in the presence of 2.5 mM MgOAc. The straight lines were determined by linear regression, fit to all data points in each region of the graph. The analysis of 56 individual reactions is presented. Open circles, raw data; red squares, average rate at each [Hop2-Mnd1].

observed here is consistent with theory (35) and with a previous study of single DNA-molecule condensation by protamine (27).

DNA condensation is dependent on the concentration of Hop2-Mnd1 (Table 1 and Fig. 2 *D*). In the absence of Hop2-Mnd1 or at $\leq$10 nM protein, the reaction is undetectable. Between 10 and 100 nM, there is a linear dependence of rate on the concentration of Hop2-Mnd1, and no significant rate increases are observed at higher protein concentrations. The protein concentration dependence observed for Hop2-Mnd1 is similar to that of other DNA condensing proteins, although significantly lower concentrations of Hop2-Mnd1 are needed to achieve the same outcome (25,27). This may be attributed to the heterodimer's high affinity for dsDNA, as well as the fact that each protein contains high numbers of positively charged residues (17% of the total number of residues for Hop2 and 20% for Mnd1; data not shown).

The condensation reaction mediated by Hop2-Mnd1 could be attributed to DNA binding that is unrelated to heterodimer function. If this is correct, then Hop2 and Mnd1 should also facilitate condensation of DNA. Therefore, to determine whether DNA condensation is specific to the Hop2-Mnd1 heterodimer, we repeated the reactions using either Hop2 or Mnd1 only. First, reactions were done in the presence of 50 nM of each protein, corresponding to the amount present in the heterodimer reaction shown in Fig. 2 *C*. The results show that neither protein is able to condense DNA when it acts alone (Table 1). Because the affinities of Hop2 and Mnd1 for DNA are lower than that of the heterodimer (18), we repeated the reactions using 100 nM of each protein, corresponding to the amount present in 200 nM heterodimer, where an efficient condensation reaction was observed to occur at a rate of 25,296 $\pm$ 7953 bp/s (Table 1). In contrast, no detectable reaction was

observed with either Hop2 or Mnd alone (Table 1). Therefore, efficient and rapid DNA condensation is intrinsic to the Hop2-Mnd1 heterodimer. These data are consistent with previous work showing that association of Hop2 with Mnd1 results in a new interface that is present only in the heterodimer and is responsible for stimulating the Dmc1 recombinase (18).

Previous computational studies suggested that histidine (modeled as imidazole) forms noncovalent interactions with free DNA nucleobases (36). Therefore, it is conceivable that the histidine tags present on Hop2 or Mnd1 could influence the DNA binding observed here. However, we do not think this is the case, as neither his_6-Hop2 nor his_6-Mnd1 bind DNA (Table 1). In sharp contrast, the his_6-Hop2/Mnd1 heterodimer binds to DNA efficiently when it is present at the same protein concentration as the individual proteins. Therefore, the histidine tags do not form the basis for the DNA condensation activity observed in this study.

Hop2-Mnd1 binds both ssDNA and dsDNA, with a preference for duplex DNA (13,16–18). To determine whether ssDNA affects the ability of Hop2-Mnd1 to condense dsDNA, single λ DNA molecules were translated into streams containing mixtures of the heterodimer and heterologous M13 ssDNA. The rate of condensation was unaffected by the presence of ssDNA, although the lag time at 300 nM Hop2-Mnd1 decreased relative to the protein-only reaction (Table 1). Thus, even though Hop2-Mnd1 can bind both ssDNA and dsDNA when simultaneously present in bulk-phase assays, ssDNA does not alter the ability of the heterodimer to condense dsDNA.

Dmc1-ssDNA/Hop2-Mnd1 filaments condense dsDNA

Hop2-Mnd1 binds to Dmc1-ssDNA nucleoprotein filaments (18), enhancing the capture of dsDNA and leading to strand invasion in vitro (21). Efficient stimulation of DNA strand invasion requires a stoichiometric ratio of Hop2-Mnd1 to Dmc1 (i.e., 1:3), with the reaction being inhibited at an excess of heterodimer relative to recombinase (see the schematic in Fig. 3) (16).

To determine whether Dmc1-ssDNA/Hop2-Mnd1 filaments condense dsDNA, single λ DNA molecules were translated into streams containing nucleoprotein filaments formed on M13 ssDNA. In separate reactions, the ratio of Hop2-Mnd1 to Dmc1 in the filaments was varied from zero to an excess of heterodimer over recombinase (Table 1).

The results show that Dmc1 nucleoprotein filaments are unable to condense dsDNA in the absence of Hop2-Mnd1, consistent with data showing that Dmc1 is inefficient at both capturing dsDNA and forming DNA networks (Figs. 1, 3, and 4, *A* and *C*). At the lowest concentration of Hop2-Mnd1 present on Dmc1 filaments (i.e., 50 nM), only one out of 18 DNA molecules condensed (Table 1). This was surprising, as this ratio of mediator to Dmc1 (i.e., 1:30) is sufficient to promote dsDNA capture (21) and this concentration of Hop2-Mnd1 is able to condense DNA in the absence of Dmc1 (Table 1). At this concentration of Hop2-Mnd1, one heterodimer is bound, on average, every 30 Dmc1 monomers. Although this spacing is sufficient for dsDNA capture, it is too far apart to permit DNA condensation.

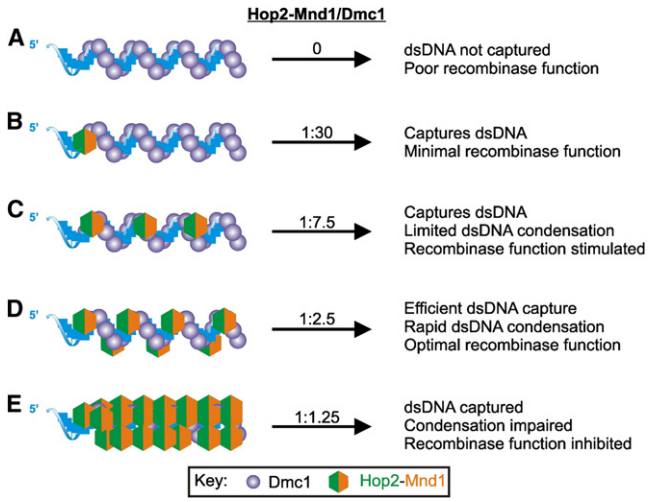

FIGURE 3 Stoichiometric amounts of Hop2-Mnd1 are required for maximal stimulation of DNA condensation and strand exchange. Five scenarios are depicted as derived from this work and previous studies (16,18,20,21): (*A*) no Hop2-Mnd1 is present, resulting in an inefficient recombinase; (*B*) a 1:30 ratio of heterodimer/Dmc1 is sufficient to capture dsDNA only ($\leq$50 nM; Table 1) (21); (*C*) substoichiometric ratios of Hop2-Mnd1 result in reduced rates of condensation and DNA strand invasion (200 nM; Table 1); (*D*) stoichiometric amounts of heterodimer produce maximal stimulation of Dmc1 or Rad51 (600 nM; Table 1) (16); and (*E*) inhibition of both condensation and DNA strand exchange are observed when an excess of heterodimer relative to recombinase is present (1200 nM; Table 1) (16).

As the concentration of heterodimer was increased to 200 nM (i.e., a ratio of 1:7.5), 100% of the DNA molecules condensed, albeit at a slower rate relative to reactions with 200 nM Hop2-Mnd1 only (Table 1 and Figs. 3 *C* and 4 *C*). Further increases in heterodimer to near-stoichiometric ratios of Hop2-Mnd1 to Dmc1 (i.e., 1:2.5), which are optimal for stimulating DNA strand invasion (16), produced a maximal condensation rate that was within experimental error, identical to that of 600 nM Hop2-Mnd1 alone (Table 1 and Fig. 4, *B* and *C*). Of importance, no lag phase was observed in the reactions containing filaments, and bright spot formation coincided with entry of the dsDNA into the reaction stream. The absence of a lag makes sense because at this concentration of heterodimer, stoichiometric amounts of Hop2-Mnd1 are presented as a collective unit by Dmc1 to the dsDNA being captured.

Further increases in Hop2-Mnd1 relative to Dmc1 to at ratio of 1:1.25 resulted in an inhibition in the rate of single DNA molecule condensation (Table 1), paralleling the inhibition of DNA strand invasion observed in bulk phase

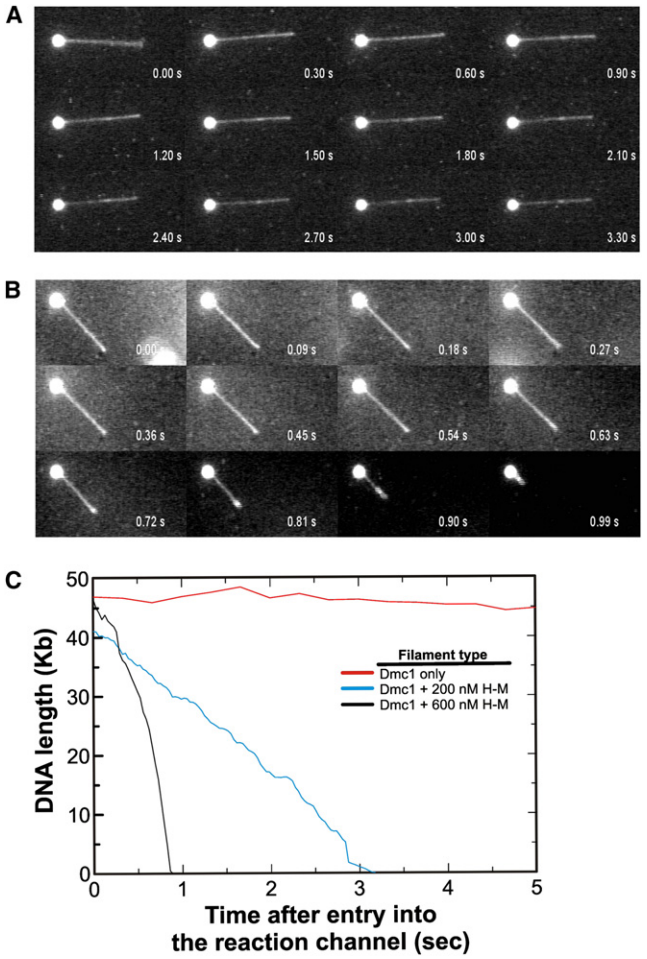

FIGURE 4 Hop2-Mnd1/Dmc1 nucleoprotein filaments condense DNA. (*A*) Selected frames from a video recording of a typical reaction between Dmc1 nucleoprotein filaments and optically trapped DNA. The reaction channel contained 1.5 μM Dmc1 and 3 μM M13 ssDNA. (*B*) Selected frames from a video recording of a representative reaction between Hop2-Mnd1/Dmc1 nucleoprotein filaments. The reaction channel contained 1.5 μM Dmc1, 3 μM M13 ssDNA, and 600 nM Hop2-Mnd1. (*C*) Analysis of the time courses shown in panels *A* and *B*. The reaction rates are given in Table 1.

(Fig. 3 *E*) (16). Under these conditions, dsDNA can still be captured into the filaments by Hop2-Mnd1 (18,21), but subsequent condensation is impeded. In addition, at this concentration of Hop2-Mnd1, free heterodimer may be present and bind to the dsDNA, further impeding the subsequent condensation of captured dsDNA. Condensation and DNA strand exchange do ultimately occur, but this requires Hop2-Mnd1 turnover from the target dsDNA, as discussed below (R. J. Pezza and R. D. Camerini-Otero, unpublished observations).

Since Hop2-Mnd1 binds Dmc1 filaments, and Dmc1-only filaments do not condense DNA, we suggest that the DNA condensation observed in these reactions results from the binding of filaments in juxtaposition along the length of the trapped dsDNA. Binding in this way can occur because a filament formed on M13 ssDNA is ~1 μm long. Thus, in principle, a single λ DNA can bind 16–18 of these filaments contiguously. Of importance, Dmc1 or Dmc1-ssDNA filaments do not condense or efficiently coaggregate DNA. Therefore, DNA condensation and stimulation of DNA network formation is intrinsic to the Hop2-Mnd1 present in the filaments. We propose, therefore, that during strand invasion, filaments first capture dsDNA, and this is immediately followed by condensation of captured DNA around the recombinase.

Condensation is stimulated by divalent metal cations

DNA condensation is affected by the type of metal ion present (25,37,38). Metal ions are also known to affect both meiotic and mitotic recombination proteins in vitro (19,39,40). To determine whether metal ions affect DNA condensation promoted by Hop2-Mnd1, reactions were performed in the presence of MgOAc, $MnCl_2$, or $CaCl_2$, or in the absence of divalent metal cations.

The results show that for Hop2-Mnd1, DNA condensation is strongly affected by the presence and type of metal ion, in the following order: $Mn^{2+} > Mg^{2+} > Ca^{2+} >$ none (Fig. 5 and Table 1). The effects are evident in both the nucleation and steady-state phases of the reactions. In the presence of Mn^{2+}, nucleation is more rapid than the temporal resolution of the system can detect. DNA condensate formation appears instantaneously with dsDNA entry into the reaction stream and is followed by rapid condensation at a rate of 45,580 $\pm$ 10,093 bp/s (Fig. 5 and Table 1). In the presence of Mg^{2+}, DNA condensates are observed after a lag of 0.23 s and condensation occurs at a slightly reduced rate of 34,068 $\pm$ 8962 bp/s. When ATP is added to Mg^{2+} reactions to mimic

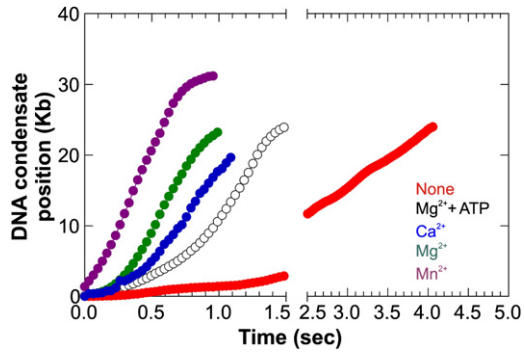

FIGURE 5 Divalent metal cations affect both nucleation and steady-state DNA condensation rates. To permit direct comparison of the reactions, the trajectories of condensation reactions for individual DNA molecules observed at each condition were averaged and normalized to the time at which formation of the DNA condensate occurred (raw data are provided in Fig. S1). The numbers of trajectories averaged were as follows: 9 for Mn^{2+}, 15 for Mg^{2+}, 11 for ATP-Mg^{2+}, 9 for Ca^{2+}, and 12 for no divalent metal ion present (none). Reaction conditions, lag times, and rates are in Table 1.

strand invasion conditions (even though ATP is not required for Hop2-Mnd1 function), the lag times for bright spot formation increase 2.7-fold to 0.62 s and the resulting condensation rate is further reduced to 29,170 ± 5803 bp/s. Although Ca^{2+} has been proposed to play an important role in effecting meiotic recombination in vitro (19,40), it is the least-effective metal ion for Hop2-Mnd1 DNA condensation, exhibiting a longer lag time for bright spot formation and slower overall condensation rate (Fig. 5 and Table 1).

Previous work showed that binding of Hop2-Mnd1 to dsDNA is unaffected by the presence of either Mg^{2+} or ATP (13). We now show that although DNA condensation does occur in the absence of a metal ion cofactor, it does so only after a sixfold longer lag phase and at a fourfold slower steady-state rate relative to Mg^{2+} (Fig. 5 and Table 1). Therefore, efficient dsDNA condensation by Hop2-Mnd1 requires divalent metal cations. The enhanced activity observed in the presence of $MnCl_2$ is due in part to this metal ion assisting Hop2-Mnd1 to efficiently overcome the rate-limiting nucleation step of DNA condensation, as explained below (41).

Hop2-Mnd1 DNA condensation is reversible

A characteristic of DNA condensation is that it is reversible once the condensing agent has been removed (27,41). It is important to determine whether this is true for Hop2-Mnd1, as decondensation would play an important role in making the DNA accessible to further DNA processing after the exchange of strands occurs. A failure to release the DNA would impair recombination.

Therefore, to determine whether Hop2-Mnd1 condensation is reversible, single DNA molecules were translated into the fluid stream containing heterodimer, and ~60% of the DNA length was allowed to condense (Fig. 6, *A* and *B*). Then, partly condensed DNA molecules were rapidly translated back into the sample fluid stream, where there was no free Hop2-Mnd1 to permit protein dissociation. As anticipated, the DNA molecules decondensed to ~85% of their initial length after they returned to the sample stream. A 100% extension relative to the reaction start point cannot be achieved, due to Mg^{2+}-dependent displacement of YOYO-1 (33). The rates of decondensation were reduced two- to threefold relative to the forward rates independently of the type of metal cation present (Fig. 6 and Fig. S2 in the Supporting Material).

Furthermore, and in contrast to forward reactions, which frequently demonstrate smooth trajectories, reverse reactions are typically discontinuous. They may have as many as five discernible phases, each persisting for various times and occurring at different rates (Fig. 6, *A* and *B*, and Fig. S2). The net effect of the discernible phases is to give the appearance of a biphasic reaction. The first phase occurs at 5586 ± 834 bp/s, with 15–50% of the DNA molecule

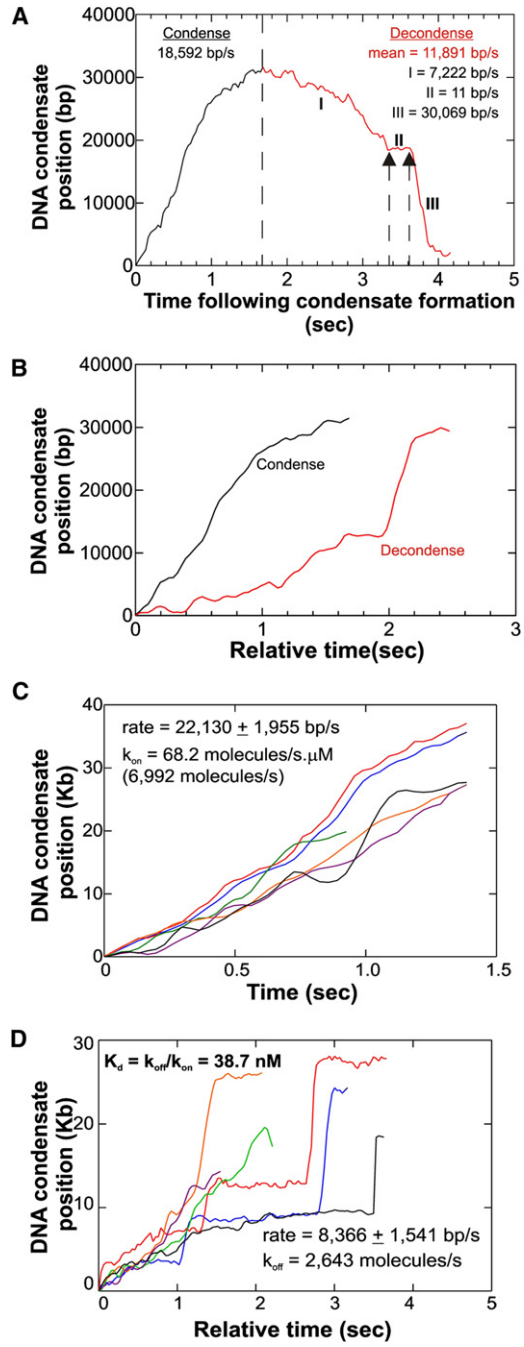

FIGURE 6 DNA condensation is reversible. (*A*) Analysis of condensation and decondensation of the same DNA molecule in the presence of 100 nM Hop2-Mnd1 and 2.5 mM MgOAc. See text for details. Black trace, condensation (forward reaction); red trace, decondensation (reverse reaction). (*B*) Normalized data of the same DNA molecule to permit direct comparison of forward and reverse reactions. (*C*) Condensation of six single molecules of DNA in the presence of 125 nM Hop2-Mnd1 and 2.5 mM MgOAc. The rate is the average for all six molecules. The on-rate, k_{on}, is calculated as described in Materials and Methods (25,27) using a site size for Hop2-Mnd1 of 3.16 (18). (*D*) Normalized data for decondensation of the same six molecules of DNA. The off-rate, k_{off}, is calculated as described in Materials and Methods (25,27).

decondensing. This is followed by a phase in which the DNA molecules rapidly undergo an ~2-fold increase in length at a rate of 48,905 ± 5351 bp/s. The first phase corresponds to a gradual dissociation of Hop2-Mnd1 from the DNA, whereas the second consists of a large-scale dissociation of Hop2-Mnd1, leading to an abrupt release of the DNA from its condensed form. For some DNA molecules, more than one rapid increase in length is observed per decondensation reaction, but each rapid jump is always preceded by a slower phase (Fig. 6 *D* and data not shown).

An analysis of six DNA molecules that were reversibly condensed under the same set of conditions demonstrates an average forward rate of 22,130 bp/s corresponding to $k_{on} = 68.2$ molecules/s.μM (Fig. 6 *C*). An analysis of the decondensation reactions of these same DNA molecules produces an average rate of 8366 bp/s corresponding to $k_{off} = 2643$ molecules/s (Fig. 6 *D*). Using these values, a K_d of 38.7 nM is obtained for Hop2-Mnd1 binding to single molecules of dsDNA. This value is 33-fold lower than the bulk phase K_d of 1.3 μM previously measured on oligonucleotide length substrates 800-fold shorter than the DNA substrate used here (18). A similar analysis of five DNA molecules was performed for reactions containing $MnCl_2$, resulting in k_{on}= 89 molecules/s.μM for forward reactions and $k_{off} = 2240$ molecules/s for reverse reactions (data not shown). This results in a K_d of 33.3 nM. Thus Mn^{2+} does not significantly alter the affinity of Hop2-Mnd1 for dsDNA; instead, it enhances the rate of binding of the heterodimer to DNA relative to other cations.

Previous studies of DNA condensation by protamine and spermatid (basic nuclear proteins) resulted in 33- to 193-fold lower single DNA-molecule K_d-values compared to Hop2-Mnd1, which ranged from 0.2 to 1.17 nM (25–27). These proteins must bind to DNA with a sufficiently high affinity to maintain the DNA in a compact state within sperm heads. Accordingly, these proteins dissociate from the DNA 11,500-fold more slowly than Hop2-Mnd1 (26). In contrast, for Hop2-Mnd1 to efficiently stimulate recombination, a lower DNA affinity and relatively rapid on- and off-rates (relative to polyamines, such as spermidine) are required. This provides a dynamic situation in the vicinity of nucleoprotein filaments. Here, dsDNA is rapidly condensed around Dmc1 or Rad51 in <2 s for 48,504 bp, facilitating DNA network formation and resulting in a more efficient homology search (23,30). Decondensation that is completed in <4 s may be required for the ensuing branch migration process or to release the DNA once recombination has been achieved. If the mediator protein binds to dsDNA with an affinity that limits access by the recombinase (or to other enzymes of recombination), then recombination may be irreversibly impeded. The rapid condensation and decondensation we observed in this study is consistent with ensemble data showing that Hop2-Mnd1 readily transfers between dsDNA molecules (20).

CONCLUSIONS

Hop2-Mnd1 stimulates meiotic homologous recombination where it binds to Dmc1 (or Rad51) nucleoprotein filaments, stabilizes them, facilitates capture of dsDNA, and then condenses dsDNA around the filament, enabling an efficient three-dimensional homology search. Maximal stimulation of dsDNA condensation and DNA strand exchange are observed at stoichiometric ratios of heterodimer to Dmc1. In addition, inhibition of both reactions is observed once an excess of Hop2-Mnd1 is present (Fig. 3) (16,18,20,21). Although the level of stimulation in DNA strand exchange reactions observed in the presence of the Hop2-Mnd1 is similar to that of Rad54, Rad54B, and the Blooms syndrome protein (BLM), the biochemical mechanism is distinct, as suggested previously (P. R. Bianco, unpublished) (13,23,42). For Rad54, which hydrolyzes ATP, dsDNA capture followed by ATP hydrolysis-coupled dsDNA translocation can be used to collapse DNA into close proximity around Rad51 nucleoprotein filaments (23). In contrast, for Hop2-Mnd1, which does not require ATP, dsDNA capture followed by DNA condensation achieves a similar outcome. Thus, Rad54 and Hop2-Mnd1 effect a common outcome using distinct biochemical mechanisms. Furthermore, these mediators provide an activity that eukaryotic recombinases lack but is present in *E. coli* RecA, namely, the ability to coaggregate DNA into three-dimensional networks. This results in a significant enhancement of DNA strand exchange mediated by Dmc1 or Rad51, as shown in this work as well as in previous studies (23,30).

SUPPORTING MATERIAL

Two figures and four movies are available at http://www.biophysj.org/biophysj/supplemental/S0006-3495(10)01316-0.

Work on this project was supported by a Susan G. Komen Breast Cancer Foundation Grant No. BCTR0601350 to P.R.B.

REFERENCES

1. Kleckner, N. 1996. Meiosis: how could it work? *Proc. Natl. Acad. Sci. USA*. 93:8167–8174.
2. Roeder, G. 1997. Meiotic chromosomes: it takes two to tango. *Genes Dev.* 11:2600–2621.
3. Bishop, D., and D. Zickler. 2004. Early decision; meiotic crossover interference prior to stable strand exchange and synapsis. *Cell.* 117:9–15.
4. Neale, M., and S. Keeney. 2006. Clarifying the mechanics of DNA strand exchange in meiotic recombination. *Nature*. 442:153–158.
5. Bishop, D., D. Park, …, N. Kleckner. 1992. DMC1: a meiosis-specific yeast homolog of *E. coli* recA required for recombination, synaptonemal complex formation, and cell cycle progression. *Cell.* 69:439–456.
6. Shinohara, A., S. Gasior, …, D. Bishop. 1997. *Saccharomyces cerevisiae* recA homologues RAD51 and DMC1 have both distinct and overlapping roles in meiotic recombination. *Genes Cells.* 2:615–629.
7. Li, Z., E. I. Golub, …, C. M. Radding. 1997. Recombination activities of HsDmc1 protein, the meiotic human homolog of RecA protein. *Proc. Natl. Acad. Sci. USA*. 94:11221–11226.

8. Masson, J., A. Davies, …, S. West. 1999. The meiosis-specific recombinase hDmc1 forms ring structures and interacts with hRad51. *EMBO J.* 18:6552–6560.
9. Masson, J., and S. West. 2001. The Rad51 and Dmc1 recombinases: a non-identical twin relationship. *Trends Biochem. Sci.* 26:131–136.
10. Hong, E., A. Shinohara, and D. Bishop. 2001. *Saccharomyces cerevisiae* Dmc1 protein promotes renaturation of single-strand DNA (ssDNA) and assimilation of ssDNA into homologous super-coiled duplex DNA. *J. Biol. Chem.* 276:41906–41912.
11. Leu, J., P. Chua, and G. Roeder. 1998. The meiosis-specific Hop2 protein of *S. cerevisiae* ensures synapsis between homologous chromosomes. *Cell.* 94:375–386.
12. Tsubouchi, H., and G. Roeder. 2002. The Mnd1 protein forms a complex with hop2 to promote homologous chromosome pairing and meiotic double-strand break repair. *Mol. Cell. Biol.* 22:3078–3088.
13. Chen, Y., C. Leng, …, T. Wang. 2004. Heterodimeric complexes of Hop2 and Mnd1 function with Dmc1 to promote meiotic homolog juxtaposition and strand assimilation. *Proc. Natl. Acad. Sci. USA.* 101:10572–10577.
14. Zierhut, C., M. Berlinger, …, F. Klein. 2004. Mnd1 is required for meiotic interhomolog repair. *Curr. Biol.* 14:752–762.
15. Henry, J., R. Camahort, …, J. Gerton. 2006. Mnd1/Hop2 facilitates Dmc1-dependent interhomolog crossover formation in meiosis of budding yeast. *Mol. Cell. Biol.* 26:2913–2923.
16. Petukhova, G., R. Pezza, …, R. Camerini-Otero. 2005. The Hop2 and Mnd1 proteins act in concert with Rad51 and Dmc1 in meiotic recombination. *Nat. Struct. Mol. Biol.* 12:449–453.
17. Enomoto, R., T. Kinebuchi, …, S. Yokoyama. 2006. Stimulation of DNA strand exchange by the human TBPIP/Hop2-Mnd1 complex. *J. Biol. Chem.* 281:5575–5581.
18. Pezza, R., G. Petukhova, …, R. Camerini-Otero. 2006. Molecular activities of meiosis-specific proteins Hop2, Mnd1, and the Hop2-Mnd1 complex. *J. Biol. Chem.* 281:18426–18434.
19. Ploquin, M., G. Petukhova, …, J. Masson. 2007. Stimulation of fission yeast and mouse Hop2-Mnd1 of the Dmc1 and Rad51 recombinases. *Nucleic Acids Res.* 35:2719–2733.
20. Chi, P., J. San Filippo, …, P. Sung. 2007. Bipartite stimulatory action of the Hop2-Mnd1 complex on the Rad51 recombinase. *Genes Dev.* 21:1747–1757.
21. Pezza, R., O. Voloshin, …, R. Camerini-Otero. 2007. Hop2/Mnd1 acts on two critical steps in Dmc1-promoted homologous pairing. *Genes Dev.* 21:1758–1766.
22. Bianco, P. R., and G. M. Weinstock. 1998. Characterization of RecA1332 in vivo and in vitro. A role for alpha-helix E as a liaison between the subunit-subunit interface and the DNA and ATP binding domains of RecA protein. *Genes Cells.* 3:79–97.
23. Bianco, P., J. Bradfield, …, A. Donnelly. 2007. Rad54 oligomers translocate and cross-bridge double-stranded DNA to stimulate synapsis. *J. Mol. Biol.* 374:618–640.
24. Neuman, K., E. Abbondanzieri, …, S. Block. 2003. Ubiquitous transcriptional pausing is independent of RNA polymerase backtracking. *Cell.* 115:437–447.
25. Brewer, L., M. Corzett, and R. Balhorn. 2002. Condensation of DNA by spermatid basic nuclear proteins. *J. Biol. Chem.* 277:38895–38900.
26. Brewer, L., M. Corzett, …, R. Balhorn. 2003. Dynamics of protamine 1 binding to single DNA molecules. *J. Biol. Chem.* 278:42403–42408.
27. Brewer, L. R., M. Corzett, and R. Balhorn. 1999. Protamine-induced condensation and decondensation of the same DNA molecule. *Science.* 286:120–123.
28. Mazin, A. V., A. A. Alexeev, and S. C. Kowalczykowski. 2003. A novel function of Rad54 protein. Stabilization of the Rad51 nucleoprotein filament. *J. Biol. Chem.* 278:14029–14036.
29. Petukhova, G., S. Stratton, and P. Sung. 1998. Catalysis of homologous DNA pairing by yeast Rad51 and Rad54 proteins. *Nature.* 393:91–94.
30. Tsang, S. S., S. A. Chow, and C. M. Radding. 1985. Networks of DNA and recA protein are intermediates in homologous pairing. *Biochemistry.* 24:3226–3232.
31. Heyer, W. D., X. Li, …, X. P. Zhang. 2006. Rad54: the Swiss Army knife of homologous recombination? *Nucl. Acids Res.* 34:4115–4125.
32. Tan, T. L., R. Kanaar, and C. Wyman. 2003. Rad54, a Jack of all trades in homologous recombination. *DNA Repair (Amst.).* 2:787–794 [erratum appears in DNA Repair (Amst). 2003 Nov 21;2(11):1293].
33. Bianco, P., L. Brewer, …, R. Baskin. 2001. Processive translocation and DNA unwinding by individual RecBCD enzyme molecules. *Nature.* 409:374–378.
34. Shaqfeh, E. S. 2005. The dynamics of single-molecule DNA in flow. *J. Non-Newt. Fluid Mech.* 130:1–28.
35. Ostrovsky, B., and Y. Bar-Yam. 1995. Motion of polymer ends in homopolymer and heteropolymer collapse. *Biophys. J.* 68:1694–1698.
36. Churchill, C., and S. Wetmore. 2009. Noncovalent interactions involving histidine: the effect of charge on pi-pi stacking and T-shaped interactions with the DNA nucleobases. *J. Phys. Chem. B.* 113:16046–16058.
37. Bloomfield, V. A. 1996. DNA condensation. *Curr. Opin. Struct. Biol.* 6:334–341.
38. Bloomfield, V. A. 1997. DNA condensation by multivalent cations. *Biopolymers.* 44:269–282.
39. Bugreev, D., and A. Mazin. 2004. Ca^{2+} activates human homologous recombination protein Rad51 by modulating its ATPase activity. *Proc. Natl. Acad. Sci. USA.* 101:9988–9993.
40. Lee, M., Y. Chang, …, T. Wang. 2005. Calcium ion promotes yeast Dmc1 activity via formation of long and fine helical filaments with single-stranded DNA. *J. Biol. Chem.* 280:40980–40984.
41. Baumann, C. G., V. A. Bloomfield, …, S. M. Block. 2000. Stretching of single collapsed DNA molecules. *Biophys. J.* 78:1965–1978.
42. Bugreev, D., O. Mazina, and A. Mazin. 2009. Bloom syndrome helicase stimulates RAD51 DNA strand exchange activity through a novel mechanism. *J. Biol. Chem.* 284:26349–26359.